Plant Biotechnology Journal

WILEY

RESEARCH ARTICLE OPEN ACCESS

A Chemical Probe for Increasing Leaf Tocopherol Levels by Coordinated Modulation of Biosynthesis, Competition and Storage

Pablo Perez-Colao[1] | Gaetan Glauser[2] | Jacobo Cruces[3] | Jorge Lozano-Juste[1] | Manuel Rodriguez-Concepcion[1]

[1]Institute for Plant Molecular and Cell Biology (IBMCP), CSIC-Universitat Politècnica de València, Valencia, Spain | [2]Neuchâtel Platform of Analytical Chemistry, University of Neuchâtel, Neuchâtel, Switzerland | [3]GalChimia S.A., Parque Empresarial de Touro, Parcelas 26-27, Fonte Díaz, A Coruña, Spain

Correspondence: Jorge Lozano-Juste (lojujo@ibmcp.upv.es) | Manuel Rodriguez-Concepcion (manuelrc@ibmcp.upv.es)

Received: 14 August 2025 | **Revised:** 17 October 2025 | **Accepted:** 29 October 2025

Funding: This work was funded by grants from the Spanish Agencia Estatal de Investigación (AEI, MICIU/AEI/10.13039/501100011033). Generalitat Valenciana, 'ERDF A way of making Europe' and 'European Union NextGeneration EU/PRTR' to MR-C (PID2020-115810GB-I00, RED2022-134577-T, PID2023-149584NB-I00 and AGROALNEXT/2022/067). JL-L (CISEJI/2022/26, CNS2023-145540, PID2021-128826OA-I00 and RYC2020-029097-I) and GalChimia (RTC-2017-6019-2). PP-C received a predoctoral fellowship from the Generalitat Valenciana (CIACIF/2021/278).

Keywords: biofortification | phytyl diphosphate | plastid | plastoglobule | tocopherol

ABSTRACT

Plant biofortification with phytonutrients typically relies on metabolic engineering strategies known as 'push' (enhancing biosynthetic flux), 'block' (inhibiting competing pathways) and 'pull' (promoting metabolite storage). Here, we describe a novel synthetic compound, X57, that simultaneously targets biosynthesis, competition and storage to enhance leaf tocopherol content. Tocopherols protect plants against oxidative stress, have a dietary value as vitamin E and are highly appreciated antioxidants in food and cosmetic formulations. X57 exerts a primary 'push' effect by inducing tocopherol biosynthesis, in part by reactivating a direct pathway that reduces geranylgeranyl diphosphate (GGPP) to phytyl diphosphate, bypassing the need for chlorophyll-derived phytol. Accordingly, X57 promotes tocopherol accumulation in etiolated seedlings and restores tocopherol synthesis in mutants deficient in phytol phosphorylation. The 'block' effect is mediated by down-regulation of GGPP consumption for carotenoid synthesis. X57 also induces a 'pull' effect via proliferation of plastoglobules (PG), plastidial lipoprotein bodies that synthesise and store tocopherols. X57-induced PG proliferation is driven by increased tocopherol levels and up-regulation of genes for PG structural proteins such as fibrillins. The unveiled genetic networks simultaneously coordinating plastidial isoprenoid metabolism and plastid differentiation might only be present in higher plants, because X57 does not promote but reduces tocopherol accumulation in *Marchantia polymorpha*.

1 | Introduction

Plastids are highly dynamic organelles capable of differentiating into different types depending on tissue-specific functions and environmental conditions. The best-known plastids are chloroplasts, which drive photosynthesis (Cackett et al. 2022). However, other plastid types accumulate particular metabolites that most often have nutritional relevance for humans. Among them, amyloplasts accumulate starch, elaioplasts contain fatty acids, chromoplasts store carotenoids such as β-carotene (provitamin A) and senescence-associated gerontoplasts accumulate tocopherols (vitamin E) (Choi et al. 2021). Besides their role as vitamins, carotenoids and tocopherols are both powerful antioxidants with health-promoting properties (Muñoz and Munné-Bosch 2019; Rodriguez-Concepcion et al. 2018). They also share the same biosynthetic origin, as they both are plastidial

isoprenoids produced from geranylgeranyl diphosphate (GGPP) precursors supplied by the methylerythritol 4-phosphate (MEP) pathway (Figure 1).

GGPP is channelled into the carotenoid pathway by the enzyme phytoene synthase (PSY), which produces phytoene in the first and main rate-determining step of the pathway (Zhou et al. 2022). Further desaturation and isomerisation steps convert non-coloured phytoene into the red carotenoid lycopene, whereas cyclisation of the ends of the linear lycopene molecule produces orange carotenes such as *β*-carotene. Oxidation of carotene rings produces yellow xanthophylls such as lutein, violaxanthin and neoxanthin (Figure 1). Tocopherols have an isoprenoid side chain produced from GGPP-derived phytyl diphosphate (phytyl-PP), and a polar chromanol head group synthesised from homogentisic acid (HGA). Both phytyl-PP and HGA are shared with other biosynthetic pathways that produce prenylquinones such as phylloquinone (vitamin K1, made from phytyl-PP and chorismate, the precursor of HGA) and plastoquinone (made from GGPP-derived solanesyl diphosphate and HGA) (Figure 1). After condensation of phytyl-PP and HGA by homogentisate phytyltransferase (also known as VITAMIN E DEFICIENT 2, VTE2), 2 methyltransferases (VTE3 and VTE4) and the tocopherol cyclase VTE1 act in different orders and combinations to generate the four tocopherols produced by plants (*δ*-, *β*-, *γ*- and *α*-, which differ in the number and position of methyl groups on their chromanol head groups). The most abundant tocopherol in *Arabidopsis thaliana* leaves is α-tocopherol, followed by much lower amounts of γ-tocopherol and virtually undetectable contents of *β*- and δ-tocopherol (Muñoz and Munné-Bosch 2019; Romer et al. 2024).

The synthesis of phytyl-PP from GGPP can occur by two possible pathways, herein referred to as the direct GGPP reduction pathway and the indirect phytol phosphorylation pathway (Dorp et al. 2015; Li, Yang, et al. 2025; Muñoz and Munné-Bosch 2019; Romer et al. 2024). The former synthesises phytyl-PP by direct reduction of GGPP by GGPP reductase (GGR). The indirect pathway involves the GGR-mediated reduction of GGPP-derived geranylgeranyl-chlorophyll to (phytyl)-chlorophyll followed by phytol hydrolysis and subsequent two-step phosphorylation to phytyl-PP (Figure 1). Phytol phosphorylation is catalysed by FARNESOL KINASE (FOLK) and VTE5, whereas VTE6 phosphorylates phytyl phosphate (phytyl-P) to produce phytyl-PP. *Arabidopsis* double mutants defective in FOLK and VTE5 or single mutants lacking VTE6 have undetectable amounts of leaf tocopherols, indicating that the phytol phosphorylation pathway provides the phytyl-PP for leaf tocopherols (Romer et al. 2024). The observation that *folk vte5* mutants contain about 40% of the phylloquinone contents found in the wild-type indicates that both the direct reduction pathway and the indirect phosphorylation pathway contribute to producing phytyl-PP for phylloquinone synthesis (Romer et al. 2024).

In chloroplasts, carotenoids, tocopherols, plastoquinone and phylloquinone are found in the envelope and in photochemically active thylakoid membranes, where they participate in photosynthesis-related processes. Tocopherols, plastoquinone and phylloquinone also accumulate in thylakoid-attached lipid bodies known as plastoglobules (PG) (Eugeni Piller et al. 2012; Morelli, Torres-Montilla, et al. 2023). PG proliferate in chloroplasts under stress conditions causing disassembly of the thylakoid membrane system (Wijk & Van Wijk and Kessler 2017). Carotenoids are found at very low levels in PG from chloroplasts but accumulate at high levels in the PG that proliferate in chromoplasts, whereas tocopherols are also abundant in the large PG present in gerontoplasts (Morelli, Torres-Montilla, et al. 2023; Muñoz and Munné-Bosch 2019; Torres-Montilla

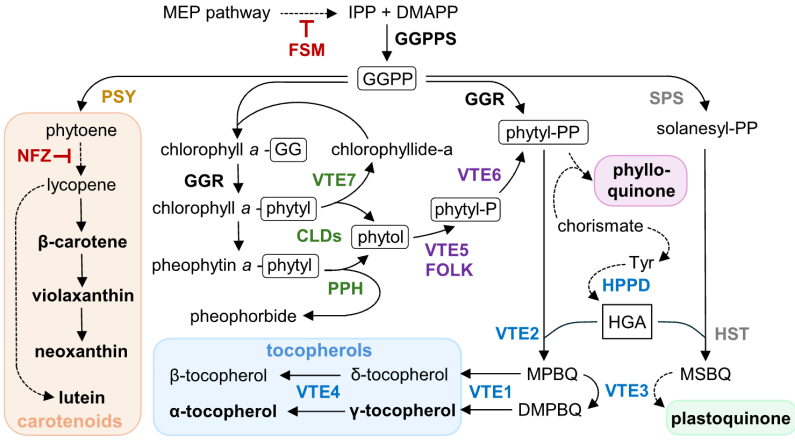

FIGURE 1 | Overview of plastidial isoprenoid metabolism. The methylerythritol 4-phosphate (MEP) pathway produces geranylgeranyl diphosphate (GGPP) for carotenoid, chlorophyll, tocopherol, plastoquinone and phylloquinone biosynthesis. Some intermediates are shared by several pathways. Phytyl diphosphate (phytyl-PP) for tocopherol and phylloquinone biosynthesis can be produced from GGPP reduction (direct pathway) or from the phosphorylation of phytol released from chlorophylls (indirect pathway). In leaves, both direct and indirect pathways supply phytyl-PP for phylloquinone biosynthesis, but only the indirect pathway is involved in tocopherol biosynthesis under normal conditions. Homogentisic acid (HGA) for tocopherol and plastoquinone biosynthesis is produced from chorismate, an intermediate that is also used in the phylloquinone biosynthetic pathway. Dashed arrows represent multiple steps. The steps targeted by fosmidomycin (FSM) and norflurazon (NFZ) are indicated in red. Enzymes are indicated in bold and their Arabidopsis accession numbers are listed in Table S1.

and Rodriguez-Concepcion 2021; Van Wijk and Kessler 2017). While controlled engineering of plastid (e.g., PG) differentiation appears as an attractive approach for biofortificación of plant tissues with health-promoting plastid-borne vitamins A, E and K1, our molecular toolbox is still quite limited (Morelli and Rodriguez-Concepcion 2023). However, it is becoming clearer that differentiation of metabolite-rich specialised plastids (e.g., chromoplasts) does not result from a set developmental programme but can occur in any plant species or tissue as a response to metabolite (e.g., carotenoid) overaccumulation (Li, Rodríguez-Concepción, and Al-Babili 2025; Llorente et al. 2020; Zheng et al. 2025). We recently showed that overexpressing *crtB*, a bacterial phytoene synthase, in leaves, resulted in a distinctive golden colour as it successfully converted chloroplasts into carotenoid-rich chromoplast-like organelles (Llorente et al. 2020; Morelli et al. 2024; Morelli, Torres-Montilla, et al. 2023). Artificial leaf chromoplasts were found to develop larger PG that accommodate high amounts of carotenoids (notably β-carotene) but also tocopherols and phylloquinone (Morelli, Torres-Montilla, et al. 2023). The new PG and membrane systems created in artificial chromoplasts proposedly improved the catalytic activity of biosynthetic enzymes (many of which are associated with PG and membranes) and the capacity to store plastidial isoprenoid phytonutrients while protecting them from degradation (Morelli, Torres-Montilla, et al. 2023). Supporting this conclusion, promoting the proliferation of PG with high-light treatments further increased the levels of carotenoids and tocopherols in *crtB*-expressing leaves (Morelli et al. 2024; Morelli, García Romañach, et al. 2023).

Although metabolic engineering approaches for the biofortification of plant tissues with carotenoids and tocopherols have been extensively studied, alternative strategies, such as the application of natural or synthetic compounds (e.g., biostimulants), remain largely unexplored (Avnee et al. 2023; Morelli and Rodriguez-Concepcion 2023). Unlike genetic engineering, this novel approach, which could be termed *chemofortification*, is reversible, dynamic, tunable on-demand and does not require alterations to the plant's genetic makeup to enhance the accumulation of health-promoting metabolites (Xu and Geelen 2018). Here, we looked for compounds able to transform the chloroplasts of *Arabidopsis* leaves into nutrient-packed organelles based on the change of the green colour characteristic of chlorophylls to the golden colour provided by carotenoids. As a result, we identified a new chemical compound, X57, that offers exceptional opportunities for chemofortification but also for studying how metabolic and developmental pathways operating in plastids are coordinated without the limitations of genetic approaches.

2 | Results

2.1 | X57 Induces a Distinctive Golden Phenotype and Tocopherol Accumulation

Changes in seedling pigmentation caused by exogenously applied compounds are commonly identified during phenotypical chemical screenings. These compounds typically cause a white (albino) or yellowish/brownish phenotype on *Arabidopsis thaliana* seedlings (Figure S1). Using seedling pigmentation as a selection strategy, we identified a particular compound (hereafter referred to as X57) that induced a distinctive golden (orange-yellow) phenotype (Figure S1), a visual indicator of altered chloroplast function and potential carotenoid overaccumulation. HPLC analysis revealed that the striking coloration of seedlings germinated and grown in the presence of X57 was associated with a marked reduction in chlorophyll content (Figure 2a). While carotenoid levels were also reduced by X57 (Figure 2a), this decrease was less pronounced than that of chlorophylls, leading to an increased carotenoid-to-chlorophyll ratio that was ultimately responsible for the golden coloration of the seedlings (Figure S2a). Importantly, X57 treatment resulted in a nearly 3-fold increase in tocopherol content, mostly resulting from *de novo* synthesis of γ–tocopherol (Figure 2a). After confirming the concentration-dependent phenotype of X57 in seedlings exposed to this compound since germination (Figure S3), we investigated whether X57 could also decrease chlorophyll and carotenoid contents and promote tocopherol accumulation in true leaves arising from seedlings not previously exposed to X57. Seedlings germinated and grown for 5 days on mock medium containing 0.05% DMSO were transferred to fresh medium containing X57. Upon transfer, the newly emerging true leaves developed the same golden phenotype observed in cotyledons of X57-germinated seedlings (Figure 2b). Metabolic profiling of whole seedlings 5 days after transferring to X57 showed reduced chlorophyll and carotenoid levels (Figure 2b) and increased carotenoid-to-chlorophyll ratio (Figure S2b). Despite the changes in photosynthetic pigment content being less pronounced than in the case of X57-germinated seedlings, the tocopherol increase in X57-transferred seedlings was similar to that observed in X57-germinated seedlings (Figure 2a,b).

2.2 | X57 Triggers the Proliferation of Plastoglobule Clusters

X57-mediated reduction in photosynthetic pigments and increase in tocopherol levels suggested a scenario of senescence. To test this possibility, we used RT-qPCR to quantify the expression of *AtORE1* and *AtSAG12* genes as markers of early and late senescence, respectively, in seedlings germinated in the presence or absence of X57. As positive controls, we used seedlings transferred to darkness to induce senescence. Neither *AtORE1* nor *AtSAG12* was up-regulated in the presence of X57 (Figure 2c), in contrast to dark-incubated seedlings, which exhibited overexpression of both genes at different time points (Figure 2d). These results indicate that X57 does not trigger a senescence-like process.

We next investigated the changes occurring in plastid ultrastructure after X57 treatment in both cotyledons and true leaves using transmission electron microscopy (TEM) (Figure 3). Cotyledons of mock-treated seedlings contained chloroplasts with only a few scattered plastoglobules (PG), whereas X57-germinated seedlings contained plastids lacking thylakoids and grana and showing a marked accumulation of small PG grouped in dense clusters (Figure 3a). Virtually identical clustered PG (cPG) were observed in the plastids present in true leaves of X57-transferred seedlings (Figure 3b). X57-associated PG proliferation (Figure 3c) was further confirmed by confocal microscopy in transgenic lines carrying the PG marker FBN7a-YFP (Vidi et al. 2007) (Figure S4).

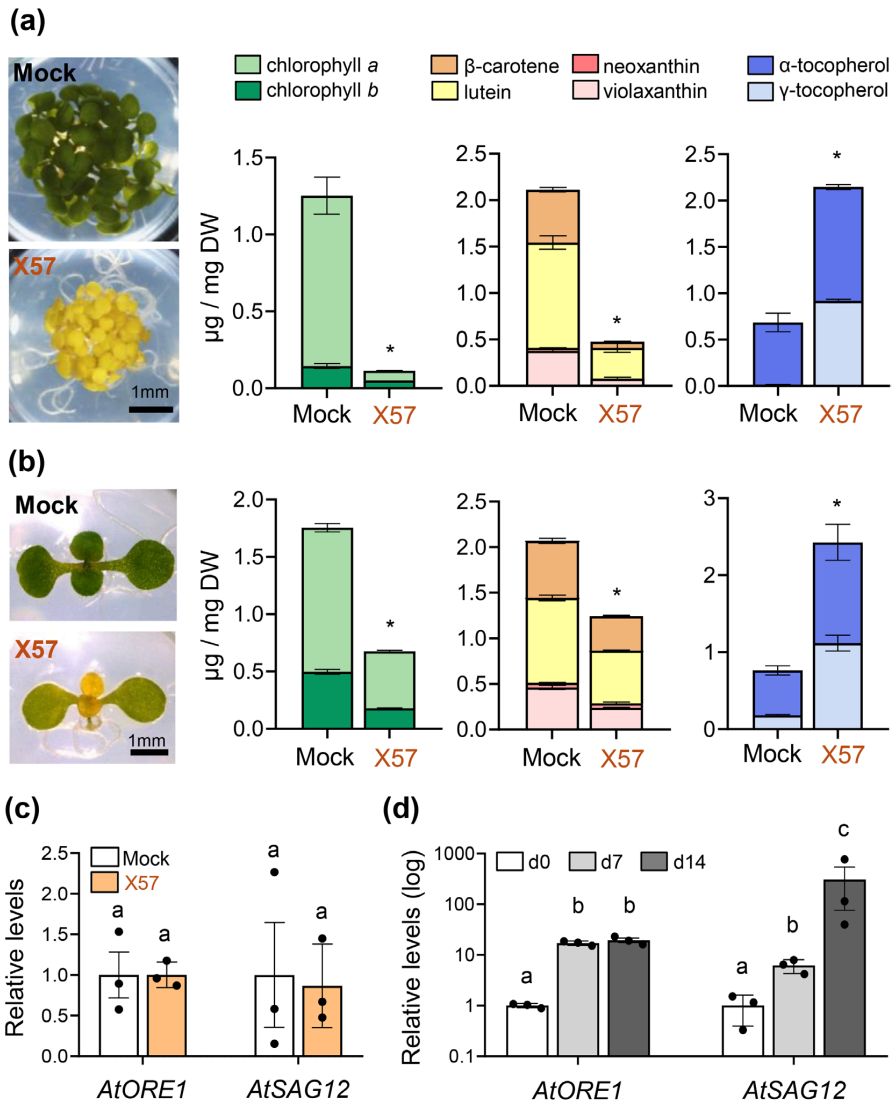

FIGURE 2 | X57 reduces chlorophyll and carotenoid levels but promotes tocopherol accumulation without triggering senescence. (a) Representative images and HPLC analysis of metabolite levels of *Arabidopsis* Col-0 seedlings germinated in MS media supplemented with 25 µM X57 or 0.05% DMSO (mock) and grown in the light for 5 days. (b) Representative images and HPLC analysis of metabolite levels of Col-0 seedlings germinated and grown for 5 days in mock medium and then manually transferred to fresh MS media supplemented with 50 µM X57 or 0.05% DMSO (mock) and incubated in the light for 5 more days. (c) Levels of *AtORE1* and *AtSAG12* transcripts quantified by RT-qPCR in Col-0 seedlings treated as described in (a). Levels are represented relative to those in mock-treated samples. (d) Levels of *AtORE1* and *AtSAG12* transcripts quantified by RT-qPCR in Col-0 seedlings germinated and grown for 5 days in mock medium (d0) and then transferred to darkness and sampled after 7 (d7) and 14 (d14) days. Levels are represented relative to those at d0 on a logarithmic scale. In all bar plots, mean ± SD of $n = 3$ independent biological replicates is represented. Asterisks and letters represent statistically significant differences ($p < 0.05$, one-way ANOVA followed by Tukey's test). In (a) and (b), statistical differences refer to total contents of chlorophylls, carotenoids or tocopherols. DW, dry weight.

2.3 | X57-Induced Tocopherol Biosynthesis Drives PG Proliferation

Besides acting as storage compartments for tocopherols and related prenyl-lipids such as plastoquinone and phylloquinone, PG are lipoprotein particles that host biosynthetic enzymes that support the synthesis of these compounds (Wijk and Van Wijk and Kessler 2017). Therefore, we could envision two non-mutually exclusive possibilities to explain the phenotype of X57-treated tissues. X57 might primarily trigger PG formation, thereby creating an optimal environment for subsequent tocopherol biosynthesis and sequestration.

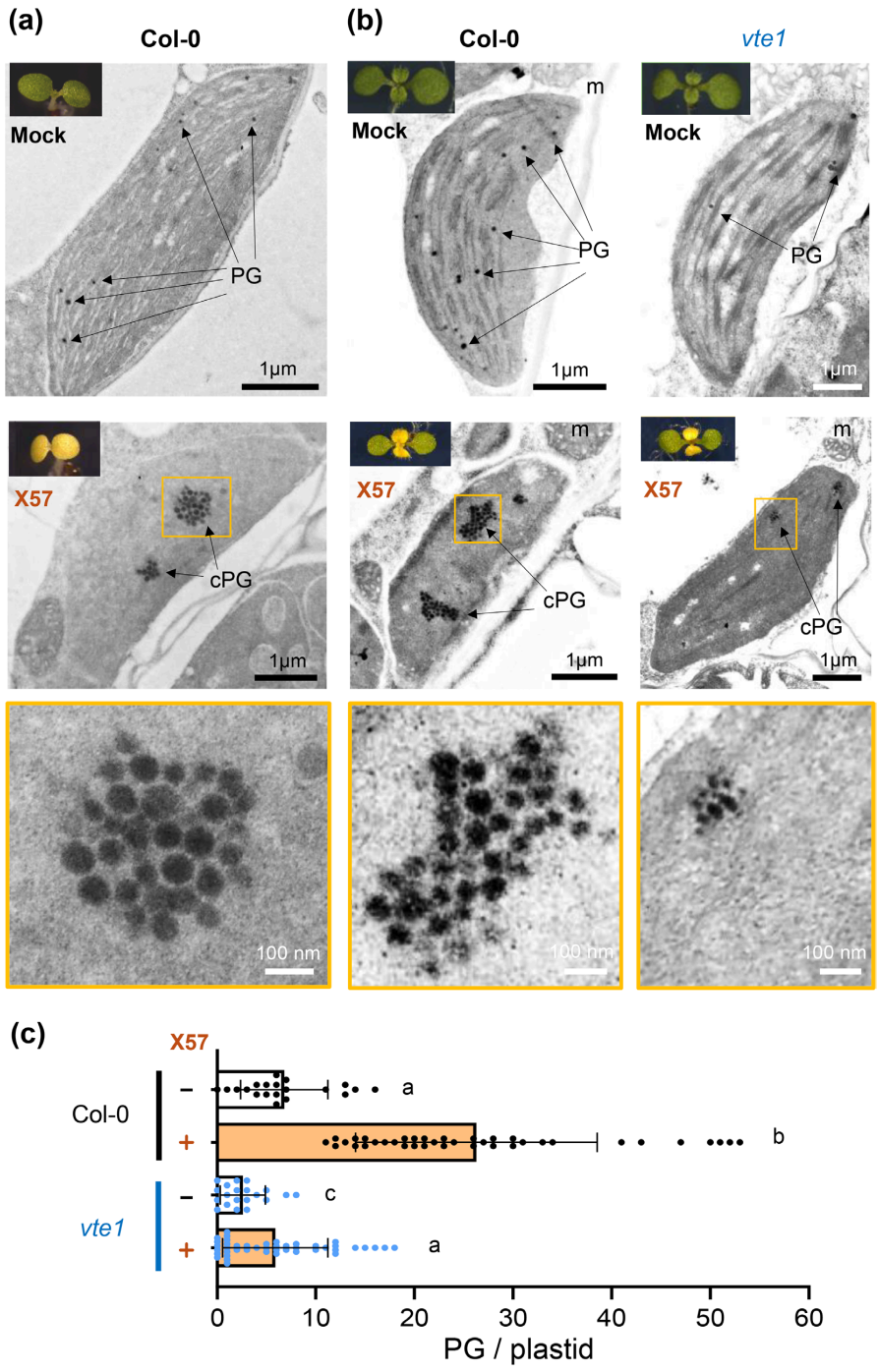

FIGURE 3 | Legend on next page.

Alternatively, X57 treatment might induce tocopherol biosynthesis to levels that would eventually result in PG proliferation. To address this question, we analysed transcriptomic changes occurring shortly (5 h) after transferring 5-day-old seedlings to either X57 or a mock control (Figure 4). RNA-seq analysis showed that X57 treatment rapidly up-regulated the expression of genes encoding PG structural proteins such as fibrillins FBN1a, FBN1b, FBN2, FBN4 and FBN8 (Figure 4

FIGURE 3 | X57 induces plastoglobule proliferation in a tocopherol-dependent manner. (a) TEM analysis of cotyledon plastids present in *Arabidopsis* Col-0 seedlings germinated in MS media supplemented with 25 μM X57 or 0.05% DMSO (mock) and grown in the light for 5 days. (b) TEM analysis of true leaf plastids present in Col-0 and *vte1* seedlings germinated and grown for 5 days in mock medium and then manually transferred to fresh MS media supplemented with 50 μM X57 or 0.05% DMSO (mock) and incubated in the light for 5 more days. In (a) and (b), inset pictures show images of the seedlings used for TEM analysis, and lower panels are magnifications of the areas boxed in orange in the central panels (X57-treated samples). (c) Quantification of plastoglobule (PG) number per plastid in Col-0 and *vte1* leaf samples from seedlings grown as described in (b). Data represent mean ± SD from at least 30 independent plastids. Letters indicate statistically significant differences ($p < 0.05$, two-way ANOVA followed by Tukey's test). PG, plastoglobules; cPG, clustered plastoglobules; m, mitochondrion.

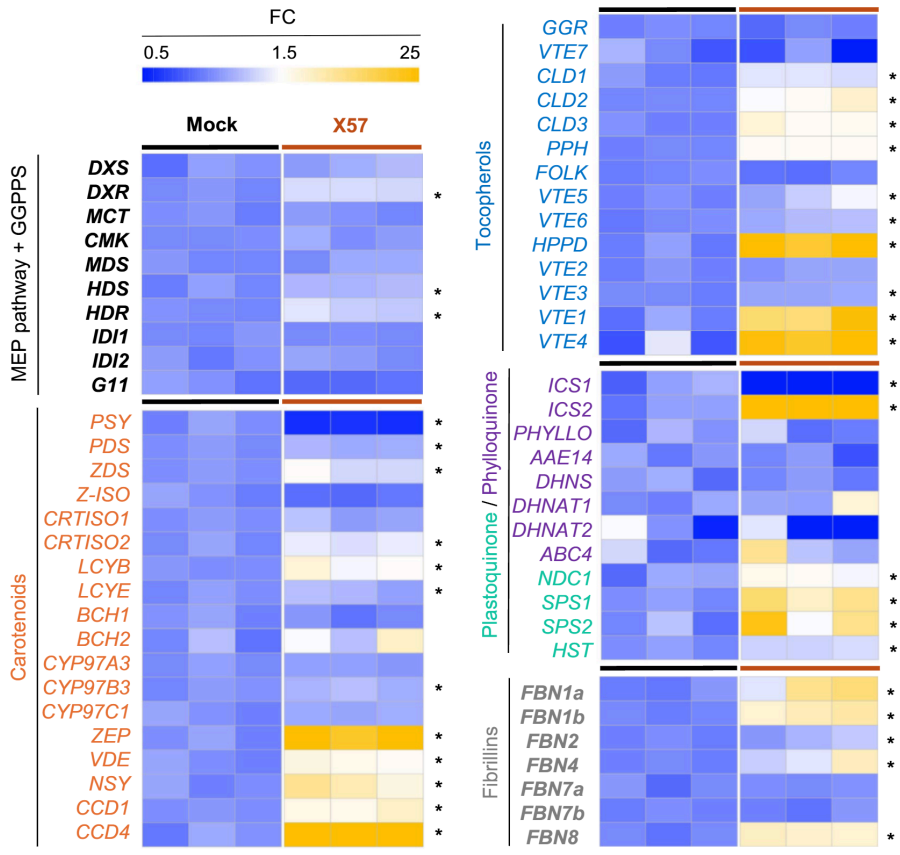

FIGURE 4 | X57 orchestrates gene expression to promote tocopherol biosynthesis and storage. Col-0 seedlings were germinated and grown for 5 days in mock medium and then manually transferred to fresh liquid MS media supplemented with 100 μM X57 or 0.05% DMSO (mock). Samples of whole seedlings were collected 5 h later and used for RNA extraction and sequencing. Heatmaps represent expression levels of genes involved in the indicated plastidial isoprenoid pathways. Columns represent biological replicates, and fold-change (FC) values were normalised using the row_scale method from the pheatmap R package. Asterisks indicate differentially expressed genes when comparing X57 and mock treatments (DESeq2; FDR ≤ 0.05). Gene accessions and transcripts per million (TPM) values are listed in Table S1, and position of the corresponding enzymes in the pathways are represented in Figure S5.

and Table S1). In the case of genes involved in tocopherol biosynthesis (Figure 1 and Figure S5), most were also induced following X57 treatment (Figure 4 and Table S1). The strongest up-regulation was observed for genes encoding enzymes involved in the production of HGA (4-hydroxyphenylpyruvate dioxygenase, HPPD) and the formation of γ-tocopherol (VTE1) and α-tocopherol (VTE4). Genes encoding PHEOPHYTINASE (PPH) or CHLOROPHYLL DEPHYTYLASE enzymes (CLD1, CLD2, CLD3), involved in the removal of phytol from chlorophylls, as well as kinases required for its phosphorylation (VTE5, VTE6), were also induced (Figures 1 and 4) (Figure S5 and Table S1).

Because transcriptomic data could not ascertain whether X57 primarily triggered tocopherol biosynthesis and then PG development or the other way around, we next analysed PG

abundance in the *vte1* mutant, which is unable to synthesise tocopherols (Kanwischer et al. 2005). Wild-type (WT) Col-0 and *vte1* mutant seeds were germinated without X57, and 5 days later some seedlings were transferred to new plates with or without X57 for 5 more days before TEM analysis of leaf chloroplast ultrastructure. Chloroplasts of mock-treated *vte1* mutant leaves showed a low number of PG compared to the WT (Figure 3b,c). PG abundance per plastid slightly increased in leaves from *vte1* seedlings transferred to X57 (Figure 3c), forming compact cPG with fewer and much smaller bodies compared to X57-treated Col-0 chloroplasts (Figure 3b). These results suggest that enhanced tocopherol biosynthesis is a major driver (but not essential) for X57-promoted cPG proliferation.

We speculated that the PG detected in *vte1* chloroplasts might result from the accumulation of PG-localised lipids other than tocopherols, including triacylglycerols, free fatty acids and/or prenylquinones such as HGA-derived plastoquinone and phytyl-PP-derived phylloquinone (Wijk and Van Wijk and Kessler 2017). To test this hypothesis, we quantified the levels of photosynthetic pigments (chlorophylls and carotenoids) and prenyl-lipids (tocopherols, plastoquinone and phylloquinone) in Col-0 and *vte1* seedlings germinated and grown for 5 days with or without X57 (Figure 5). Chlorophyll and carotenoid levels in *vte1* seedlings remained comparable to those in the WT Col-0 background and responded similarly to X57 treatment (Figure 5a). As expected, tocopherols were undetectable in the mutant even in the presence of X57 (Figure 5a). In the case of both plastoquinone and phylloquinone, *vte1* seedlings showed a WT phenotype in terms of basal content under control conditions and, unexpectedly, decreased levels in X57-treated samples (Figure 5a). In contrast to that described for tocopherols, the striking X57-triggered reduction in plastoquinone and phylloquinone levels did not parallel changes in biosynthetic gene expression. Genes specifically involved in plastoquinone biosynthesis, including those encoding solanesyl diphosphate synthase (*SPS1* and *SPS2*) and homogentisate solanesyltransferase (*HST*) (Figure 1) were not repressed but up-regulated (Figure 4). In the case of phylloquinone, only the genes encoding the two enzyme paralogs for the first step of the pathway, *ICS1* and *ICS2* (Figure S5), showed significantly altered expression, but in mutually opposite directions (Figure 4 and Table S1). We therefore conclude that the limited cPG proliferation observed in X57-treated *vte1* seedlings (Figure 3) is not supported by enhanced plastoquinone or phylloquinone synthesis. On the contrary, plastoquinone and phylloquinone contents

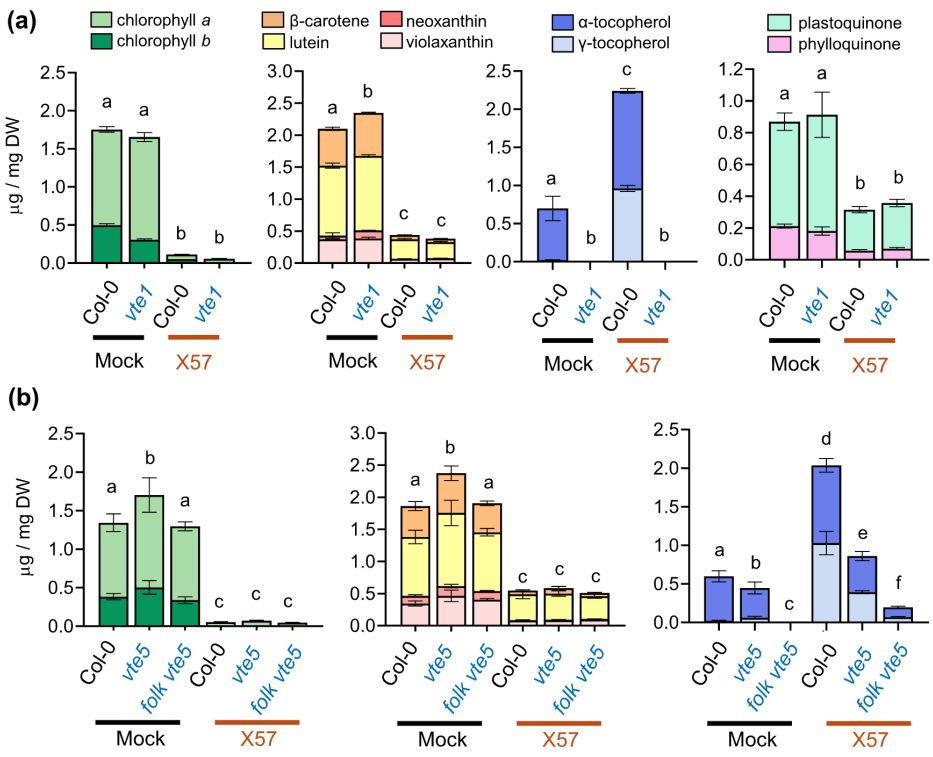

FIGURE 5 | X57 reactivates the direct pathway for phytyl-PP production. (a) Quantification of plastidial isoprenoid levels of Col-0 and *vte1* seedlings germinated in MS media supplemented with 25 µM X57 or 0.05% DMSO (mock) and grown in the light for 5 days. (b) HPLC analysis of plastidial isoprenoid levels of Col-0 and mutants defective in phytol phosphorylation (single *vte5* and double *folk vte5*) germinated and grown as described in (a). Bar plots represent mean ± SD of $n = 6$ (a) or $n = 3$ (b) independent biological replicates. Letters indicate statistically significant differences ($p < 0.05$) according to post hoc Tukey's tests following two-way ANOVA. DW, dry weight.

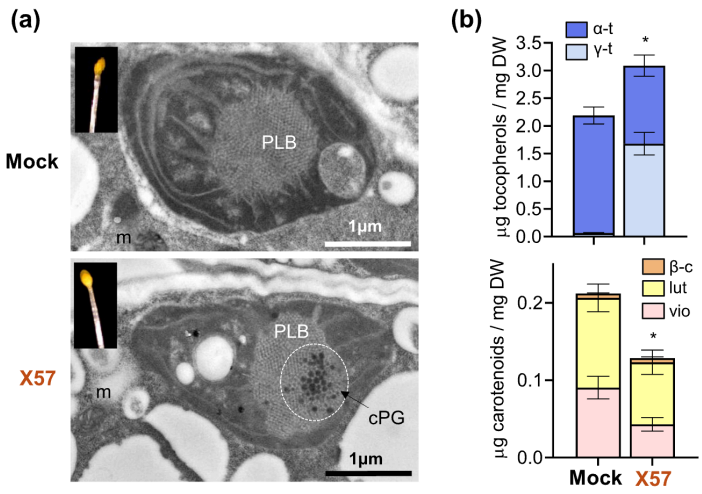

FIGURE 6 | X57 induces plastoglobule proliferation in etiolated seedlings. (a) TEM analysis of cotyledon plastids present in Col-0 seedlings germinated in MS media supplemented with 25 µM X57 or 0.05% DMSO (mock) and grown in the dark for 5 days. Inset pictures show images of the seedlings used for TEM analysis. PLB, prolamellar body; cPG, clustered plastoglobules; m, mitochondrion. (b) HPLC analysis of the seedlings described in (a). Mean ± SD of $n = 3$ independent biological replicates is shown. Asterisks represent statistically significant differences ($p < 0.05$) according to post hoc Tukey's tests following one-way ANOVA. DW, dry weight. α-t, α-tocopherol. γ-t, γ-tocopherol; β-c, β-carotene; lut, lutein; vio, violaxanthin.

are reduced by X57 treatment by a mechanism independent of biosynthetic gene expression.

2.4 | X57-Induced Tocopherol Biosynthesis Does Not Exclusively Rely on Phytol Recycling

After confirming that X57 promotes tocopherol production and PG proliferation, we next focused on the biosynthetic pathway. Phytyl-PP for leaf tocopherol biosynthesis appears to derive from the indirect phytol phosphorylation pathway (Romer et al. 2024). Among other enzymes, this process is dependent on the kinases FOLK and VTE5 (Figure 1), which phosphorylate the phytol moiety released from chlorophyll breakdown (Dorp et al. 2015; Mène-Saffrané, 2018; Romer et al. 2024). Based on this information, it was hypothesised that the observed increase in tocopherols following X57 treatment should be reduced in the single *vte5* mutant and completely prevented in the double *folk–vte5* mutant, which shows significantly lower or absent tocopherol contents, respectively (Dorp et al. 2015; Romer et al. 2024). Surprisingly, X57 treatment promoted tocopherol accumulation in both *vte5* and *folk vte5* mutant seedlings (Figure 5b), indicating that X57 is able to produce tocopherols *de novo* even in the absence of a functional phytol phosphorylation pathway. Similar to tocopherol-deficient *vte1* seedlings (Figure 5a), levels of chlorophylls and carotenoids in *vte5* and *folk vte5* mutants showed a WT response to X57 treatment (Figure 5b).

Supporting the conclusion that X57-promoted tocopherol biosynthesis can proceed independent of chlorophyll-derived phytol supply, etiolated seedlings grown with X57 lacked chlorophylls but showed a marked rise in PG number and tocopherol levels, specifically γ-tocopherol, while retaining normal etioplast ultrastructure (Figure 6). Interestingly, carotenoid levels were reduced in X57-treated etiolated seedlings (Figure 6b), similar to that observed in light-grown seedlings treated with X57 (Figures 2 and 5). The observation that the X57-dependent decrease in carotenoid levels is independent of the presence of chlorophylls but tocopherol-associated suggests that it might be caused by diversion of GGPP from carotenoid to tocopherol production via the X57-reactivated direct phytyl-PP biosynthesis pathway (Figure 1). Consistently, reduced GGPP supply by inhibition of the MEP pathway with fosmidomycin (FSM) (Rodríguez-Concepción 2010) did not alter total tocopherol levels in the absence of X57 but it significantly reduced tocopherol accumulation in X57-germinated seedlings (Figure 7a). These results suggest that at least part of the phytyl-PP required for the X57-promoted boost in tocopherol biosynthesis comes from GGPP synthesised *de novo* by the operation of the MEP pathway (Figure 1). Furthermore, changes in tocopherol levels were paralleled by PG abundance (Figure 7b,c), again supporting the conclusion that tocopherol accumulation is the main determinant of X57-promoted PG proliferation.

2.5 | X57-Triggered Transcriptional Reprogramming Diverts Precursors to Tocopherol Biosynthesis

Based on the described results, we hypothesised that redirecting GGPP from competing pathways like carotenoid biosynthesis might increase phytyl-PP biosynthesis for tocopherol production even in etiolated seedlings lacking chlorophylls. To test this possibility, we used norflurazon (NFZ), an inhibitor of phytoene desaturation in the second step of the carotenoid pathway (Figure 1) (Ortiz-Alcaide et al. 2019). As anticipated, NFZ treatment of

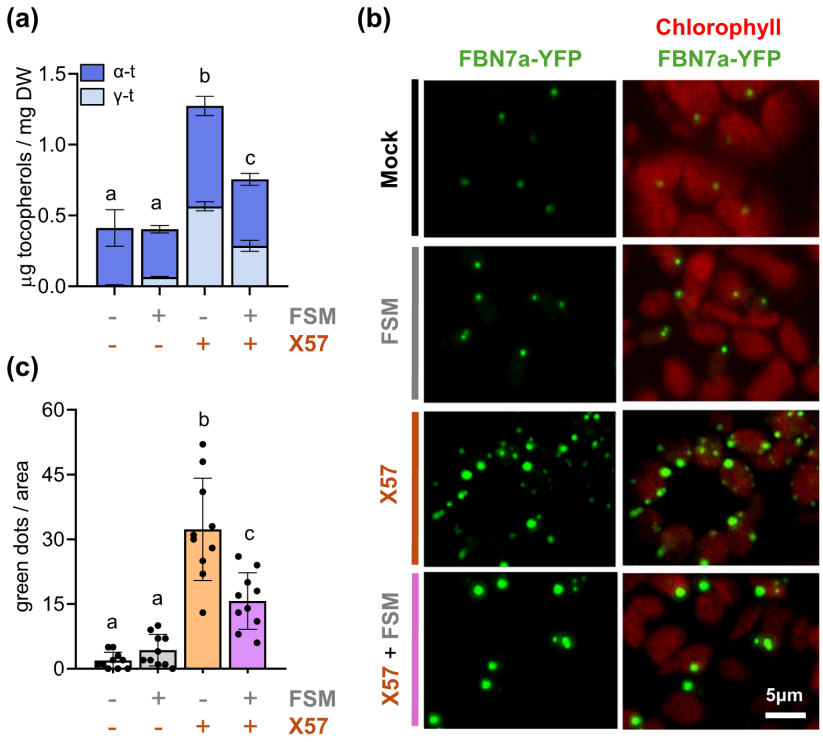

FIGURE 7 | X57-triggered tocopherol production is inhibited by blocking MEP-derived GGPP synthesis. (a) HPLC analysis of tocopherol levels of Col-0 seedlings germinated in MS media supplemented with 25 µM X57, 50 µM fosmidomycin (FSM), both, or 0.05% DMSO (mock) and grown in the light for 5 days. Mean ± SD of $n = 3$ independent biological replicates are represented. DW, dry weight. α-t, α-tocopherol. γ-t, γ-tocopherol. (b) *35S:FBN7a-YFP* seedlings were germinated and grown for 5 days in mock medium and then manually transferred to fresh MS media supplemented with 50 µM X57, 100 µM FSM, both, or 0.05% DMSO (mock) and incubated in the light for 5 more days. Panels show confocal images of the distribution of the fluorescent PG marker FBN7a-YFP (green) and chlorophyll (red) in leaves of the transgenic seedlings. (c) Quantification of PG number (green fluorescent dots) in the samples described in (b). Mean ± SD of measurements of 10 independent leaf areas are shown. Letters indicate statistically significant differences ($p < 0.05$) according to one-way ANOVA followed by Tukey's post hoc test.

etiolated seedlings caused the accumulation of phytoene (which is virtually undetectable under normal conditions) and a strong reduction in downstream carotenoid levels (Figure 8a). In etiolated seedlings germinated with both NFZ and X57, total carotenoid levels were further reduced (Figure 8a). Tocopherol levels in NFZ-treated seedlings remained unchanged compared to mock controls, indicating that blocking carotenoid biosynthesis alone is insufficient to enhance tocopherol production. However, the combined treatment with X57 and NFZ resulted in a moderate (about 30%) yet significant increase in tocopherol levels relative to X57 alone (Figure 8a). Altogether, the data suggest that, besides up-regulating tocopherol biosynthetic genes, X57 likely promotes a specific diversion of MEP-derived GGPP flux towards tocopherol biosynthesis.

Examination of RNA-seq data showed that genes for flux-controlling enzymes of the MEP pathway (Rodríguez-Concepción 2010) were moderately up-regulated in X57-treated seedlings (Figure 4, Figure S5 and Table S1), consistent with a presumably higher supply of precursors for GGPP synthesis. While many carotenoid biosynthetic genes were also up-regulated, the gene encoding phytoene synthase (PSY) was strongly down-regulated (Figure 4) (Table S1). PSY uses GGPP in the first and main rate-determining step of the carotenoid pathway (Figure 1), and its down-regulation is expected to cause a bottleneck resulting in reduced carotenoid levels even if the rest of the pathway genes are up-regulated (Zhou et al. 2022). We therefore speculated that X57 might divert GGPP precursors for direct phytyl-PP biosynthesis and downstream tocopherol production by repressing *PSY* expression. To test our model and, at the same time, enrich leaves in both tocopherols and carotenoids, we applied X57 to *Nicotiana benthamiana* leaves that transiently expressed a bacterial phytoene synthase (crtB) able to bypass the eventual repression of the endogenous *PSY* genes. *Nicotiana* leaves were agroinfiltrated with constructs to produce crtB or GFP (as a control), and after 2 days, the leaf was infiltrated with X57 or a mock control. Three days later (i.e., 5 days after agroinfiltration), X57 treatment led to a yellowish colour in GFP-infiltrated areas compared to mock-treated controls (Figure 8b). Metabolite analysis of GFP control areas found that X57 reduced chlorophyll and carotenoid levels enough to explain the yellowish appearance but to a lesser extent than in *Arabidopsis* seedlings (compare Figures 2b and 8b). Interestingly, the

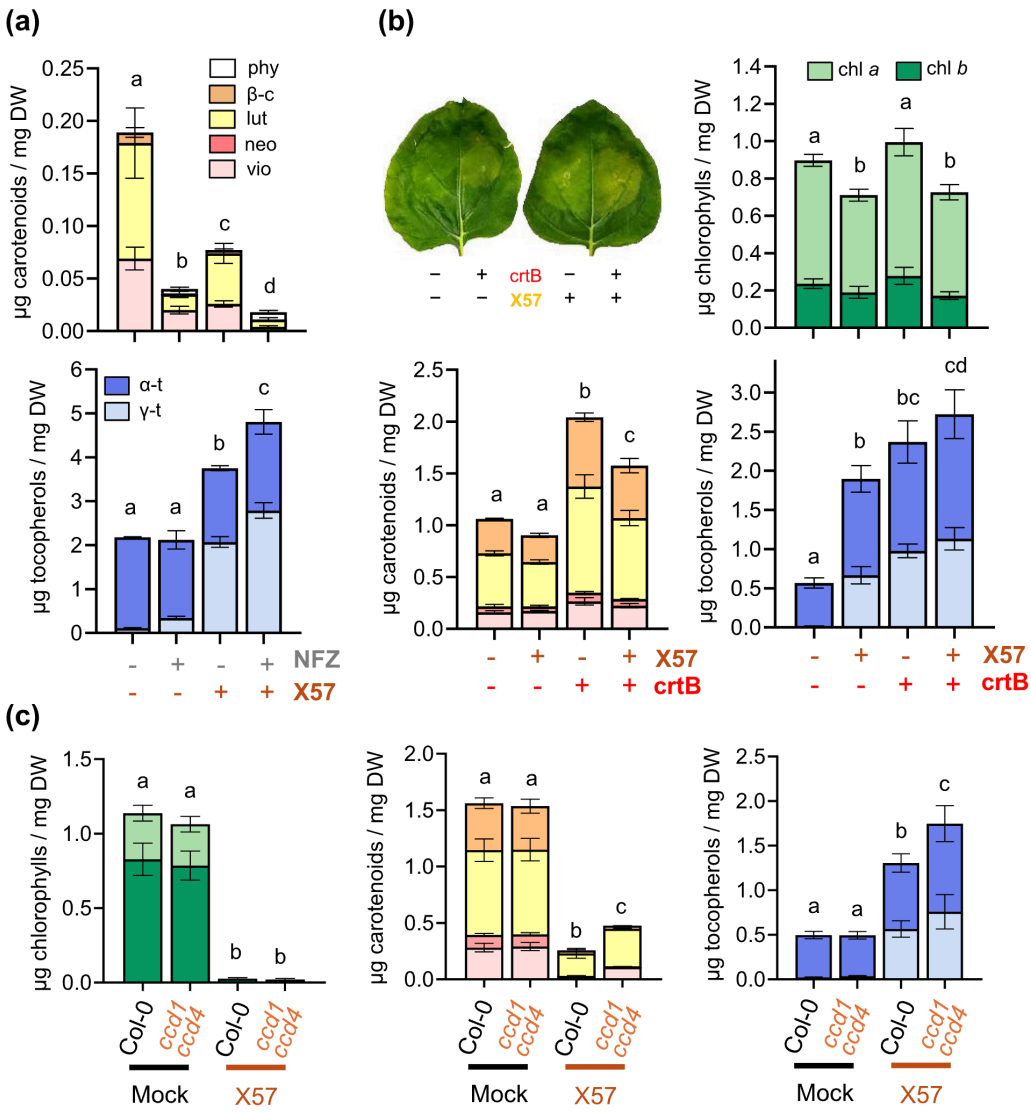

FIGURE 8 | Alterations of the carotenoid pathway impact X57-dependent tocopherol accumulation. (a) HPLC analysis of carotenoid and tocopherol levels of Col-0 seedlings germinated in MS media supplemented with 25 µM X57, 0.2 µM norflurazon (NFZ), both, or 0.05% DMSO (mock) and grown in the dark for 5 days. (b) Leaves from 3-week-old *Nicotiana benthamiana* plants were agroinfiltrated with constructs to express *crtB* (or *GFP* as a control) and 2 days later the same areas were infiltrated with 100 µM X57 or 0.1% DMSO (mock). Images show representative leaves 5 days after agroinfiltration (3 days after X57 or mock treatment). Samples from these leaves were collected for HPLC analysis of plastidial isoprenoid levels. (c) HPLC analysis of plastidial isoprenoid levels of Arabidopsis Col-0 and mutant seedlings defective in carotenoid degradation (*ccd1 ccd4* double mutant) germinated in MS media supplemented with 25 µM X57 or 0.05% DMSO (mock) and grown in the light for 5 days. Plots show mean ± SD of $n = 3$ independent biological replicates. Letters indicate statistically significant differences ($p < 0.05$) according to two-way ANOVA followed by Tukey's post hoc test. DW, dry weight; phy, phytoene; β-c, β-carotene; lut, lutein; neo, neoxanthin; vio, violaxanthin; α-t, α-tocopherol; γ-t, γ-tocopherol.

X57-promoted increase in total tocopherol accumulation was similar in both systems. As expected, agroinfiltration of crtB led to increased tocopherol accumulation (Morelli, Torres-Montilla, et al. 2023), whereas the presence of both crtB and X57 additively promoted vitamin E enrichment (Figure 8b). The orange colour associated with crtB activity was visually stronger in crtB-agroinfiltrated areas treated with X57 (Figure 8b). This visual phenotype was not due to increased carotenoid production but likely due to decreased chlorophyll levels in crtB + X57 compared to crtB areas (Figure 8b). Most importantly, higher carotenoid accumulation but similar chlorophyll levels were observed in crtB + X57 compared to X57 alone (Figure 8b), confirming that the blockage of carotenoid production detected in X57-treated leaves can be reverted by

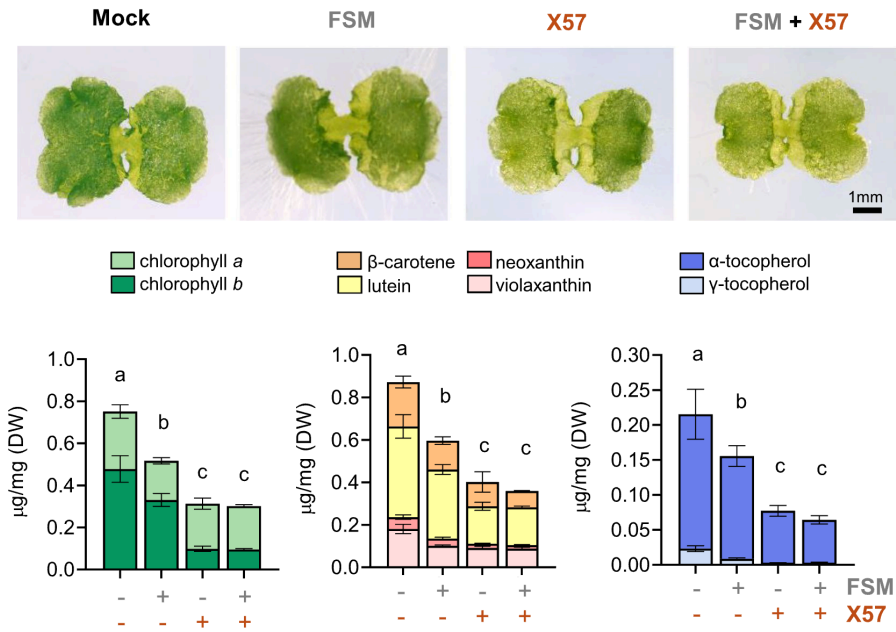

FIGURE 9 | X57 does not induce but decreases tocopherol accumulation in *Marchantia polymorpha*. Upper panels show representative images of *Marchantia polymorpha* Tak-1 thalli grown for 10 days on Gamborg B5 medium supplemented with 25 µM X57, 50 µM FSM, a combination of both, or a mock solution (0.05% DMSO). Bar plots correspond to the HPLC analysis of their plastidial isoprenoid content. Letters indicate statistically significant differences ($p < 0.05$) according to one-way ANOVA followed by Tukey's post hoc test.

providing extra phytoene synthase activity. Yet the observation that X57 infiltration reduced carotenoid contents in crtB areas suggests additional mechanisms repressing carotenoid accumulation in X57-treated leaves. Indeed, further examination of our RNA-seq data revealed that X57 treatment caused 1.5- and 7-fold up-regulation of genes encoding carotenoid cleavage enzymes CCD1 and CCD4, respectively (Figure 4, Figure S5 and Table S1). Loss of these carotenoid-degrading enzymes in the Arabidopsis double mutant *ccd1 ccd4* resulted in an attenuated down-regulation of carotenoid levels (and higher tocopherol accumulation) compared to WT controls in response to X57 treatment (Figure 8c). These findings suggest that both *PSY* down-regulation and enhanced carotenoid cleavage might contribute to X57-mediated carotenoid suppression.

2.6 | X57-Mediated Tocopherol Accumulation Is Not Conserved in Bryophytes

The reported results suggest that X57 might be developed as a chemofortification tool to improve vitamin E levels in plants by enhancing tocopherol biosynthetic gene expression, providing extra precursors diverted from competing pathways and improving sequestering capacity in PG. Bryophytes are emerging as promising chassis organisms for the development of metabolic biofactories (Lindström Battle and Sweetlove 2025; Nowaczyński et al. 2025). They synthesise many different specialised secondary metabolites, including isoprenoids. In particular, the liverwort *Marchantia polymorpha*, one of the best-studied bryophytes due to a growing toolkit of genetic resources for metabolic engineering, has been shown to produce carotenoids and phytol (Nowaczyński et al. 2025; Takemura and Misawa 2021). Because the *Marchantia* genome contains homologues of enzymes involved in tocopherol biosynthesis (Figure S6), we tested whether the addition of X57 to the growth medium could also have a tocopherol-promoting effect in this organism. X57 reduced the levels of *Marchantia* chlorophylls and carotenoids (Figure 9), similar to that shown for X57-treated *Arabidopsis* and *Nicotiana* plants. However, tocopherol accumulation was not promoted but reduced by X57 in *Marchantia* (Figure 9). Treatment with FSM also resulted in decreased levels of chlorophylls, carotenoids and tocopherols, and it did not exacerbate the effect of X57 (Figure 9), suggesting that both compounds interfere with the same pathways in *Marchantia*. The observation that tocopherol levels were not increased by X57 in *Marchantia* suggests that the X57-activated molecular pathways leading to tocopherol accumulation might be conserved in higher plants such as *Arabidopsis* and *Nicotiana* but missing or diverged in *Marchantia*.

3 | Discussion

In this study, we introduce the synthetic small molecule X57 as a promising chemical tool to (i) understand the mechanisms regulating the accumulation of tocopherols and (ii) enrich leaves with vitamin E. Biotechnological strategies for the nutritional enrichment, that is, biofortification, of plant tissues include three main approaches (Morelli and

Rodriguez-Concepcion 2023). The 'push' approach involves the overexpression of biosynthetic enzymes that catalyse bottleneck steps to promote metabolic flux and facilitate the accumulation of downstream metabolites. The 'block' approach aims to inhibit competing steps in the pathway, improving channelling towards the production of the target metabolites. Finally, the 'pull' approach focuses on enhancing the cellular storing capacity for those metabolites, hence promoting their accumulation. Our data indicate that X57 treatment leads to vitamin E enrichment of leaves by uniquely combining the three ('push', 'block' and 'pull') effects.

X57 has a primary 'push' activity by inducing tocopherol synthesis, in part via rapid up-regulation of tocopherol biosynthetic genes (Figure 4). Interestingly, X57 treatment caused a preferential increase in γ-tocopherol in leaves (Figures 2, 5, 6, 7 and 8). Photosynthetic tissues mostly accumulate α-tocopherol, whereas γ-tocopherol is more abundant in seeds (Li, Yang, et al. 2025; Muñoz and Munné-Bosch 2019). Beyond serving as a precursor of α-tocopherol, γ-tocopherol may have specific yet poorly understood physiological functions. It has been proposed to scavenge lipid peroxyl radicals and reactive nitrogen species more efficiently than α-tocopherol, suggesting a specialised role under stress (Abbasi et al. 2007). Consistently, γ-tocopherol increases not only by treatment with X57 but also with other inhibitors causing photooxidative stress such as FSM or NFZ, even without changes in total tocopherol levels (Figures 7a and 8a). Although all tocopherol forms are classified as vitamin E, γ-tocopherol has demonstrated stronger anti-inflammatory and anti-cancer properties in mammalian cell models (Es-Sai et al. 2025).

Interestingly, our data demonstrate that the extra tocopherols that accumulate in cotyledons and leaves upon X57 treatment are produced, at least in part, using phytyl-PP provided by a pathway that is not active or used for tocopherol biosynthesis under normal conditions. Recent data demonstrated that the production of tocopherols in *Arabidopsis* leaves relies on the indirect phytyl-PP supply pathway, that is, on phytol phosphorylation (Romer et al. 2024). However, treatment with X57 appeared to reactivate a direct pathway for phytyl-PP production that might normally provide precursors for phylloquinone biosynthesis (Figure 1). Several lines of evidence support this conclusion. First, the X57-dependent increase in tocopherol accumulation is independent of chlorophyll levels. Similar increases in tocopherol contents were found in X57-germinated and X57-transferred *Arabidopsis* seedlings, despite chlorophyll reduction being much stronger in the former (Figure 2). In *Nicotiana*, X57 infiltration boosted the tocopherol content of leaves despite a modest decrease in chlorophyll levels (Figure 8b). Most strikingly, the lack of chlorophylls in etiolated *Arabidopsis* seedlings, which only accumulate non-phytylated chlorophyll precursors such as protochlorophyllide, did not prevent the X57-dependent up-regulation of tocopherol accumulation (Figures 6 and 8a). Further evidence was provided by pharmacological treatments. Inhibition of GGPP supply with FSM (Figure 1) strongly reduced X57-dependent tocopherol accumulation (Figure 7a), suggesting that at least part of the phytyl-PP required to produce tocopherols comes from the direct GGPP reduction pathway. The third, strongest line of evidence supporting a pathway independent of phytol phosphorylation for X57-promoted phytyl-PP supply came from the analysis of *Arabidopsis* mutants. In particular, double *folk vte5* mutants were devoid of tocopherols in the absence of X57 but produced them when exposed to X57 (Figure 5b).

While X57 is a synthetic molecule, it is very likely that activation of the direct phytyl-PP supply pathway could also occur under physiological conditions, in particular tissues or in response to specific environmental cues. In any case, the signalling pathway triggered by X57 appears to be missing in *Marchantia* (Figure 9). In this bryophyte, X57 does not promote but down-regulates tocopherol content, paralleling the repressing effect on chlorophyll and carotenoid accumulation that is also observed in *Arabidopsis* and *Nicotiana* leaves. We speculate that the observed decrease in chlorophyll and carotenoid levels detected in X57-treated tissues might be due, at least in part, to X57-dependent regulation of gene expression (Figure 4). In the case of chlorophylls, X57 treatment rapidly activates the expression of genes encoding chlorophyll dephytylases (CLDs and PPH), likely contributing to removing chlorophylls by a senescence-independent process (Figure 2c). For carotenoids, the drop caused by X57 appears to be due to multiple reasons, as detailed below, and it might also indirectly contribute to chlorophyll degradation. Indeed, specific blocking of the carotenoid pathway with NFZ reduces carotenoid but also chlorophyll levels (Ortiz-Alcaide et al. 2019), and mutants unable to produce carotenoids are albino because they also fail to accumulate chlorophylls (Rodriguez-Concepcion et al. 2018).

The 'block' effect of X57 further contributes to devote metabolic precursors to tocopherol biosynthesis. Only a few hours after exposing *Arabidopsis* seedlings to X57, the expression of *PSY* drops while other genes of the carotenoid pathway are up-regulated (Figure 4). A reduction in PSY activity is expected to consume less GGPP for carotenoid biosynthesis, which then would become available for GGR-mediated reduction to produce phytyl-PP (Figure 1). Consistently, providing extra PSY activity by transiently expressing *crtB* in *Nicotiana* leaves can partially revert the negative effects that X57 treatment has on carotenoid contents (Figure 8b). X57 also up-regulates the expression of genes for carotenoid-degrading enzymes, CCD1 and CCD4 (Figure 4), whereas X57-triggered carotenoid loss is attenuated in double mutant *ccd1 ccd4* seedlings (Figure 8c). These results support the conclusion that enzymatic degradation contributes to the X57-mediated reduction in carotenoid levels. Interestingly, CCD4 is associated with PG in *Arabidopsis* leaves, where it cleaves β-carotene, lutein and violaxanthin (Rottet et al. 2016). Because X57 treatment leads to a proliferation of PG (Figures 3 and 7b), it is possible that this compound sequentially causes a block in phytoene production by repressing *PSY*, the conversion of the remaining phytoene into β-carotene and xanthophylls such as lutein and violaxanthin by up-regulating the expression of downstream biosynthetic genes, and the degradation of PG-accumulated carotenoids by inducing *CCD4* gene expression.

In addition to carotenoids, X57 treatment also causes a reduction in plastoquinone and phylloquinone (Figure 5a) despite the block of the carotenoid pathway and the activation of the MEP pathway presumably resulting in increased supply of GGPP for the production of solanesyl-PP and phytyl-PP (Figure 1) and the amount of PG (a prime storage compartment for prenyl-lipids) is also increased. In this case, the changes in metabolite levels are hardly explained by the effect of X57 on biosynthetic gene

expression (Figure 4). Instead, the drop in plastoquinone and phylloquinone accumulation might be due to competition for substrates. Phylloquinone is formed from the condensation of phytyl-PP and a chorismate-derived moiety, whereas plastoquinone is made from solanesyl-PP and HGA (Figure 1). While the supply of phytyl-PP is activated by X57, it might not be readily available for phylloquinone biosynthesis, for example, by efficient channelling into the tocopherol pathway. An activated flux into the tocopherol pathway might also prevent the formation of solanesyl-PP for plastoquinone biosynthesis and deplete part of the phytyl-PP pool normally used for phylloquinone production. Additionally, the strong up-regulation of the gene encoding HPPD by X57 (Figure 4) suggests that the production of HGA from chorismate might be induced, again providing more substrate for vitamin E biosynthesis and depleting precursors for plastoquinone production (Figure 1). Regardless of the specific mechanisms involved, it is clear that X57 favours tocopherol biosynthesis partly by exerting a 'block' effect that prevents precursor consumption by competing pathways (e.g., carotenoid, plastoquinone and phylloquinone pathways).

A third crucial feature of X57 for tocopherol enrichment is a 'pull' effect caused by the proliferation of PG. Our results together support the conclusion that X57-induced PG proliferation is mostly driven by enhanced tocopherol synthesis. Genetic evidence supporting this conclusion came from the analysis of the *vte1* mutant, in which the lack of tocopherols was associated with fewer and smaller PG (Figure 3). Additionally, reducing tocopherol biosynthesis in WT seedlings treated with FSM and X57 led to substantially lower proliferation of PG compared to those treated with X57 alone (Figure 7b). However, the observation that PG proliferation is also induced by X57 in tocopherol-depleted *vte1* seedlings (Figure 3) suggests that other mechanisms besides tocopherol overaccumulation contribute to the PG phenotype of X57-treated plastids. Indeed, the up-regulation of fibrillin-encoding genes soon after X57 application (Figure 4) indicates that PG proliferation might also be actively promoted. Also, X57-promoted PG cluster in large groups of small electron-dense bodies (Figure 3), a distinctive trait that is not present in other tocopherol-overaccumulating plastids such as gerontoplasts or chromoplasts, including crtB-induced artificial leaf chromoplasts (Llorente et al. 2020; Morelli, Torres-Montilla, et al. 2023). PG clustering occurs upon overexpression of PG-associated fibrillins such as FBN1 (Rey et al. 2000) and FBN7 (Li et al. 2023), suggesting that X57-associated clustered PG (cPG) might primarily result from the up-regulation of genes for PG structural fibrillins. The cPG found in X57-treated tissues resemble those formed during light-triggered etioplast-to-chloroplast differentiation (Solymosi and Aronsson 2013). Similar cPG are also observed in mutants impaired in chloroplast differentiation, such as those lacking plastid-encoded RNA polymerase-associated proteins (PAPs), which are essential for activating the transcription of plastid genes required for thylakoid biogenesis (Ahrens et al. 2025; Arsova et al. 2010; Garcia et al. 2008; Myouga et al. 2008; Vergara-Cruces et al. 2024). In these undifferentiated plastids, PG may serve as storage sites for lipophilic metabolites such as tocopherols. We propose that the combined effect of X57 causing a higher production of tocopherols but a lower accumulation of chlorophylls and carotenoids eventually prevents thylakoid formation and forces tocopherols to accumulate at high levels within cPG. The observation that X57 prevents thylakoid formation even in the absence of tocopherols, as in the *vte1* mutant (Figure 5a), further supports the conclusion that this compound impacts photosynthetic pigment accumulation and plastid differentiation independently of tocopherol production. Interestingly, the increased accumulation of tocopherols in X57-treated *ccd1 ccd4* seedlings (Figure 8c) suggests that carotenoid removal from PG by X57-up-regulated CCD4 might provide extra sites to accommodate increased tocopherol contents.

The enrichment of plant tissues with tocopherols is a major goal of plant metabolic engineering (Li, Yang, et al. 2025). In addition to their plant protection and dietary value as vitamin E, tocopherols are extensively used as chemical antioxidants in food and cosmetic formulations. The main biotechnological attempts to date aimed at tocopherol biofortification focused on increasing the flux of the biosynthetic pathway in non-photosynthetic tissues. Only some recent attempts have combined 'push' and 'pull' strategies in leaves using crtB and environmental treatments to promote PG proliferation (Morelli, García Romañach, et al. 2023). Here, we report a completely new tool (X57) and method (chemofortification) that combines a 'triple effect' to improve between 2- and 3-fold the vitamin E content of plant leaves. Besides reactivating a direct pathway for phytyl-PP production and up-regulating the expression of tocopherol biosynthetic genes in leaves to 'push' the metabolic flux towards the production of vitamin E, X57 is able to 'block' the consumption of common precursors by competing pathways (carotenoids, plastoquinone and phylloquinone) and has a 'pull' effect as it promotes the proliferation of PG that accommodate tocopherols and prevent their degradation. Besides the applied role of X57 as a bioestimulant targeting health-promoting tocopherols, its use as a research tool has shown the existence of common signalling pathways and gene networks controlling the production of tocopherols in coordination with precursor availability (by pushing supply pathways and blocking competing pathways) and storage capacity (by developing sequestering structures) in higher plants. Further studies should determine the precise molecular mechanism by which X57 orchestrates gene expression eventually resulting in the observed metabolic and structural (plastid differentiation) effects.

4 | Materials and Methods

4.1 | Plant Material, Chemical Treatments and Growth Conditions

All *Arabidopsis thaliana* lines used in this study were in the Columbia (Col) background, including the PGL34-YFP marker line, here referred to as *35S:FBN7a-YFP* (Vidi et al. 2007), and the mutants *ccd1 ccd4* (Llorente et al. 2020), *vte1* (Kanwischer et al. 2005), *vte5* and *folk vte5* (Romer et al. 2024). Seeds were surface-sterilised with 70% ethanol for 5 min, followed by 100% ethanol for 1 min, and then air-dried. Unless indicated otherwise, sterile seeds were directly sown onto solid Murashige and Skoog (MS) medium with 1% sucrose and without vitamins in 24-well square cell culture plates or 9 cm Petri dishes. When indicated, the medium was supplemented with different concentrations of X57 or with 0.05% DMSO as a mock control. X57 belongs to a proprietary screening library from GalChimia and

it was provided directly by them and diluted in DMSO to prepare a 50 mM stock solution. Fosmidomycin (Sigma-Aldrich) and norflurazon (Zorial, Syngenta) were diluted in water (Ortiz-Alcaide et al. 2019) and added to the medium in some experiments. Stratification was carried out at 4°C in darkness for 3 days. Then, plates were incubated in a growth chamber at 22°C under long-day (LD) conditions of 8 h of darkness and 16 h of fluorescent white light, with a Photosynthetic Photon Flux Density (PPFD) of 100 $\mu mol\, m^{-2} s^{-1}$. For transfer experiments, seedlings germinated on mock MS medium and grown for 5 days in the LD chamber and then transferred to fresh MS plates. For RNA-seq experiments, 5-day-old seedlings were transferred to liquid medium and incubated in the LD chamber (during the day period) for 5 h. For etiolation assays, plates with seeds were illuminated for 5 h following stratification (to synchronise germination) and then incubated at 22°C in complete darkness for 5 days. For dark-induced senescence experiments, plates with 5-day-old seedlings were incubated at 22°C in complete darkness for up to 2 weeks. *Nicotiana benthamiana* plants used for transient expression assays were grown in a greenhouse under a LD photoperiod of 8 h of darkness (at 21°C) and 16 h of light with a PPFD of 100 $\mu mol\, m^{-2} s^{-1}$ (at 26°C). *Marchantia polymorpha* Tak-1 thalli were propagated from gemmae and cultivated on solid Gamborg B5 medium supplemented with 1% sucrose. Thalli were grown in the same LD chamber used for *Arabidopsis*.

4.2 | Metabolite Extraction and Quantification

Chlorophylls, carotenoids and tocopherols were extracted from 2–4 mg of lyophilised tissue. Powdered samples were mixed in 2 mL Eppendorf tubes with 375 µL methanol and 25 µL of a 10% (*w/v*) canthaxanthin (Sigma-Aldrich) solution in chloroform as an internal standard. Samples were vortexed for 10 s and then disrupted with a TissueLyser II (QIAGEN) using 4 mm glass beads at 30 Hz. After 1 min, 400 µL Tris-NaCl (pH 7.5) were added, followed by a second round of lysis, the addition of 800 µL chloroform and a final 1 min lysis step. Following centrifugation for 10 min at 13000 rpm and 4°C, the organic phase (lower) was collected, dried using a SpeedVac (Eppendorf Concentrator Plus) for 1 h and resuspended in 150 µL acetone. Resuspended samples were sonicated for 15 s and filtered through 0.2 µm filters into amber vials. A volume of 10 µL was injected into an Agilent 1200 HPLC system equipped with a YMC C30 reverse-phase column and operated with a methanol/water/tert-butyl methyl ether gradient. Chlorophylls and carotenoids were detected using a photodiode array (PDA) detector at specific wavelengths (280 nm for phytoene, 470 nm for the rest of carotenoids and 650 nm for chlorophylls), whereas tocopherols were detected using a fluorescence detector (excitation at 290 nm, emission at 330 nm). Peak areas were normalised to the canthaxanthin internal standard and dry weight, and metabolite quantification was performed by comparison with commercial standards using the Agilent ChemStation software levels. When comparing wild-type and *vte1* mutant seedlings, tocopherols, plastoquinone (PQ-9) and phylloquinone were quantified by UHPLC-QTOF-MS as described (Morelli, Torres-Montilla, et al. 2023) with minor adjustments. In brief, prenyl-lipids were extracted from 10 mg lyophilised tissues with 1 mL THF:MeOH:H_2O (50:50:15) and the resulting mixture was further diluted 10-fold before injection into an Acquity UPLC I-Class (Waters) equipped with an Acquity BEH C18 (2.1 × 50 mm, Waters) and pure water and methanol as mobile phases A and B, respectively. The column temperature was set to 75°C. A gradient of 85%–100% B followed by an isocratic hold at 100% B was applied. The flow rate was 0.8 mL/min. The injection volume was 0.3 µL. Detection was performed by MS/MS using a QTRAP 6500+ (Sciex) operated in negative atmospheric pressure chemical ionisation. Specific MRM transitions optimised for each compound were used. A calibration curve weighted by 1/x was built from standard concentrations at 10, 20, 100, 500, 1000 and 2000 ng/mL.

4.3 | Electron Microscopy

For transmission electron microscopy (TEM) analysis, cotyledon and true leaf samples were fixed in a solution containing 2.5% (*w/v*) paraformaldehyde and 0.5% (*w/v*) glutaraldehyde, followed by three 5 min washes in 0.1 M phosphate-buffered saline (PBS). Post-fixation was performed by incubating the samples in 2% osmium tetroxide for 2 h, followed by three additional 5 min washes with distilled water. Dehydration was conducted stepwise at increasing temperatures (30°C, 50°C, 70°C and 90°C), and infiltration was carried out using ethanol–LR White resin mixtures of increasing concentration (1:2–1:1) at 90°C. Samples were then immersed in 100% LR White resin for 1–24 h, embedded in gelatin capsules and polymerised at 60°C for 48 h. Ultrathin sections were obtained using holey grids. Contrast staining was performed sequentially with 2% (*w/v*) uranyl acetate for 9 min, followed by lead citrate for 9 min. Sections were visualised using an HT7800 120 kV transmission electron microscope (Hitachi Ltd., Tokyo, Japan), and images were acquired with a 20 MP CMOS XAROSA digital camera (EMSIS GmbH, Münster, Germany). Plastoglobule number was recorded and quantified using ImageJ.

4.4 | Confocal Microscopy

Yellow fluorescent protein (YFP) and chlorophyll autofluorescence were visualised using a Zeiss 780 confocal laser scanning microscope. Excitation was performed with an argon laser at 488 nm. Emission was detected using a 450–490 nm filter for YFP and a 610–700 nm filter for chlorophyll autofluorescence. Fluorescent YFP spots were quantified using ImageJ.

4.5 | RNA Isolation and Sequencing

Total RNA was extracted from approximately 4 mg of ground, freeze-dried tissue using the PureLink RNA Mini Kit (Thermo Scientific), following the manufacturer's instructions. RNA integrity was assessed using an Agilent 2100 Bioanalyzer, and only samples with an RNA Integrity Number (RIN) ≥ 7 were used for sequencing (RNA-seq) by BGI Tech Solutions (https://services.bgi.com) using the DNBSEQ platform. Reads were aligned to the *Arabidopsis thaliana* reference genome (GCF_000001735.4_TAIR10.1; TAIR10), with an average alignment rate of 97.93%. Gene expression quantification and identification of differentially expressed genes (DEGs) were performed using the default DrTom analysis pipeline provided by BGI. Heatmaps were created using the pheatmap package in RStudio

(Kolde 2018). Transcripts per million (TPM) values for selected genes are listed in Table S1. Raw sequencing data are deposited at the Gene Expression Omnibus (GEO) under accession number GSE303753.

4.6 | Quantitative Real-Time PCR

RNA concentration was measured with a NanoDrop spectrophotometer (Thermo Scientific), and integrity was verified by agarose gel electrophoresis. First-strand cDNA synthesis was performed using either the Transcriptor First Strand cDNA Synthesis Kit (Roche) or the NZY First-Strand cDNA Synthesis Kit (NZYtech), following the respective manufacturers' protocols. The resulting cDNA was used as a template for RT-qPCR reactions carried out in 20 μL volumes using the LightCycler 480 SYBR Green I Master Mix (Roche) on a QuantStudio 3 (Applied Biosystems) thermocycler. Relative gene expression was calculated using *UBC21* (At5g25760) as a reference gene. Primers used are listed in Table S2.

4.7 | Transient Expression

Three-week-old *Nicotiana* plants were agroinfiltrated as described (Andersen et al. 2021) with *Agrobacterium tumefaciens* GV3101 strains transformed with crtB and GFP constructs previously available in the lab (Llorente et al. 2020). After 2 days, agroinfiltrated leaf areas were infiltrated with 100 μM ×57 or a 0.1% DMSO mock solution. Samples were collected 5 days after agroinfiltration (3 days after treatment).

4.8 | BLAST Analysis

Arabidopsis protein sequences retrieved from UniProt were used as input queries in a BLASTp search against the *Marchantia polymorpha* Tak-1 reference proteome (version 7.1) using SequenceServer (version 2.0.0). Searches were performed using an E-value threshold of 1e-20.

Acknowledgements

We thank Felix Kessler (University of Neuchatel) for the *35S:FBN7a-YFP* line, Peter Dörmann and Katharina Gutbrod (University of Bonn) for providing seeds of the *vte5* mutants, and Miguel Ángel Blázquez and Macarena Mellado-Sánchez (IBMCP) for providing *Marchantia polymorpha* thalli. We are also grateful to José M. Pérez-Beser and Esther Pau-Ramos (IBMCP) for general technical support, Maria T. Mínguez (University of Valencia SCSIE Microscopy Section) for her expert support with TEM, Javier Forment (IBMCP Bioinformatics platform) for his assistance with RNA-seq and BLAST analyses, and the IBMCP Metabolomics platform staff for help with HPLC.

Conflicts of Interest

The authors declare no conflicts of interest.

Data Availability Statement

The data that support the findings of this study are available in the Supporting Information of this article.

References

Abbasi, A. R., M. Hajirezaei, D. Hofius, U. Sonnewald, and L. M. Voll. 2007. "Specific Roles of α- and γ-Tocopherol in Abiotic Stress Responses of Transgenic Tobacco." *Plant Physiology* 143, no. 4: 1720–1738. https://doi.org/10.1104/PP.106.094771.

Ahrens, F. M., P. F. V. do Prado, H. S. Hillen, and T. Pfannschmidt. 2025. "The Plastid-Encoded RNA Polymerase of Plant Chloroplasts." *Trends in Plant Science* 30, no. 7: 712–723. https://doi.org/10.1016/J.TPLANTS.2025.01.010.

Andersen, T. B., B. Llorente, L. Morelli, et al. 2021. "An Engineered Extraplastidial Pathway for Carotenoid Biofortification of Leaves." *Plant Biotechnology Journal* 19, no. 5: 1008–1021. https://doi.org/10.1111/PBI.13526.

Arsova, B., U. Hoja, M. Wimmelbacher, et al. 2010. "Plastidial Thioredoxin z Interacts With Two Fructokinase-Like Proteins in a Thiol-Dependent Manner: Evidence for an Essential Role in Chloroplast Development in Arabidopsis and Nicotiana Benthamiana." *Plant Cell* 22, no. 5: 1498–1515. https://doi.org/10.1105/TPC.109.071001.

Avnee, M., S. Sood, D. R. Chaudhary, P. Jhorar, and R. S. Rana. 2023. "Biofortification: An Approach to Eradicate Micronutrient Deficiency." *Frontiers in Nutrition* 10: 1233070. https://doi.org/10.3389/FNUT.2023.1233070.

Cackett, L., L. H. Luginbuehl, T. B. Schreier, E. Lopez-Juez, and J. M. Hibberd. 2022. "Chloroplast Development in Green Plant Tissues: The Interplay Between Light, Hormone, and Transcriptional Regulation." *New Phytologist* 233, no. 5: 2000–2016. https://doi.org/10.1111/NPH.17839.

Choi, H., T. Yi, and S. H. Ha. 2021. "Diversity of Plastid Types and Their Interconversions." *Frontiers in Plant Science* 12: 692024. https://doi.org/10.3389/FPLS.2021.692024/PDF.

Dorp, K. V., G. Hölzl, C. Plohmann, et al. 2015. "Remobilization of Phytol From Chlorophyll Degradation Is Essential for Tocopherol Synthesis and Growth of Arabidopsis." *Plant Cell* 27, no. 10: 2846–2859. https://doi.org/10.1105/TPC.15.00395.

Es-Sai, B., H. Wahnou, S. Benayad, et al. 2025. "Gamma-Tocopherol: A Comprehensive Review of Its Antioxidant, Anti-Inflammatory, and Anticancer Properties." *Molecules* 30, no. 3: 653. https://doi.org/10.3390/MOLECULES30030653.

Eugeni Piller, L., M. Abraham, P. Dörmann, F. Kessler, and C. Besagni. 2012. "Plastid Lipid Droplets at the Crossroads of Prenylquinone Metabolism." *Journal of Experimental Botany* 63, no. 4: 1609–1618. https://doi.org/10.1093/JXB/ERS016.

Garcia, M., F. Myouga, K. Takechi, et al. 2008. "An Arabidopsis Homolog of the Bacterial Peptidoglycan Synthesis Enzyme MurE Has an Essential Role in Chloroplast Development." *Plant Journal* 53, no. 6: 924–934. https://doi.org/10.1111/J.1365-313X.2007.03379.X.

Kanwischer, M., S. Porfirova, E. Bergmüller, and P. Dörmann. 2005. "Alterations in Tocopherol Cyclase Activity in Transgenic and Mutant Plants of Arabidopsis Affect Tocopherol Content, Tocopherol Composition, and Oxidative Stress." *Plant Physiology* 137, no. 2: 713–723. https://doi.org/10.1104/PP.104.054908.

Kolde, R. 2018. "Pheatmap: pretty heatmaps. R package v.1.0.12. [WWW document]." https://CRAN.R-project.org/package=pheatmap.

Li, J., D. Kong, T. Song, et al. 2023. "OsFBN7-OsKAS I Module Promotes Formation of Plastoglobules Clusters in Rice Chloroplasts." *New Phytologist* 239, no. 5: 1771–1789. https://doi.org/10.1111/nph.19081.

Li, L., M. Rodríguez-Concepción, and S. Al-Babili. 2025. "Update on Carotenoid and Apocarotenoid Metabolisms and Functions in Plants." *Plant Physiology* 198, no. 4: kiaf304. https://doi.org/10.1093/PLPHYS/KIAF304.

Li, Y., D. Yang, Y. Ren, et al. 2025. "Vitamin E in Plants: Biosynthesis Pathways, Biofortification Strategies, and Regulatory Dynamics."

International Journal of Molecular Sciences 26, no. 7: 3380. https://doi.org/10.3390/IJMS26073380.

Lindström Battle, A. L., and L. J. Sweetlove. 2025. "Bryophytes as Metabolic Engineering Platforms." *Current Opinion in Plant Biology* 85: 102702. https://doi.org/10.1016/j.pbi.2025.102702.

Llorente, B., S. Torres-Montilla, L. Morelli, et al. 2020. "Synthetic Conversion of Leaf Chloroplasts Into Carotenoid-Rich Plastids Reveals Mechanistic Basis of Natural Chromoplast Development." *Proceedings of the National Academy of Sciences of the United States of America* 117, no. 35: 21796–21803. https://doi.org/10.1073/PNAS.2004405117/-/DCSUPPLEMENTAL.

Morelli, L., L. García Romañach, G. Glauser, V. Shanmugabalaji, F. Kessler, and M. Rodriguez-Concepcion. 2023. "Nutritional Enrichment of Plant Leaves by Combining Genes Promoting Tocopherol Biosynthesis and Storage." *Metabolites* 13, no. 2: 193. https://doi.org/10.3390/METABO13020193.

Morelli, L., P. Perez-Colao, D. Reig-Lopez, X. Di, B. Llorente, and M. Rodriguez-Concepcion. 2024. "Boosting Pro-Vitamin A Content and Bioaccessibility in Leaves by Combining Engineered Biosynthesis and Storage Pathways With High-Light Treatments." *Plant Journal* 119, no. 6: 2951–2966. https://doi.org/10.1111/TPJ.16964.

Morelli, L., and M. Rodriguez-Concepcion. 2023. "Open Avenues for Carotenoid Biofortification of Plant Tissues." *Plant Communications* 4, no. 1: 100466. https://doi.org/10.1016/J.XPLC.2022.100466.

Morelli, L., S. Torres-Montilla, G. Glauser, V. Shanmugabalaji, F. Kessler, and M. Rodriguez-Concepcion. 2023. "Novel Insights Into the Contribution of Plastoglobules and Reactive Oxygen Species to Chromoplast Differentiation." *New Phytologist* 237, no. 5: 1696–1710. https://doi.org/10.1111/NPH.18585.

Muñoz, P., and S. Munné-Bosch. 2019. "Vitamin E in Plants: Biosynthesis, Transport, and Function." *Trends in Plant Science* 24, no. 11: 1040–1051. https://doi.org/10.1016/J.TPLANTS.2019.08.006.

Myouga, F., C. Hosoda, T. Umezawa, et al. 2008. "A Heterocomplex of Iron Superoxide Dismutases Defends Chloroplast Nucleoids Against Oxidative Stress and Is Essential for Chloroplast Development in Arabidopsis." *Plant Cell* 20, no. 11: 3148–3162. https://doi.org/10.1105/TPC.108.061341.

Nowaczyński, F., R. Nicoletti, B. Zimowska, and A. Ludwiczuk. 2025. "*Marchantia Polymorpha* as a Source of Biologically Active Compounds." *Molecules* 30, no. 3: 558. https://doi.org/10.3390/MOLECULES30030558.

Ortiz-Alcaide, M., E. Llamas, A. Gomez-Cadenas, A. Nagatani, J. F. Martínez-García, and M. Rodríguez-Concepción. 2019. "Chloroplasts Modulate Elongation Responses to Canopy Shade by Retrograde Pathways Involving hy5 and Abscisic Acid." *Plant Cell* 31, no. 2: 384–398. https://doi.org/10.1105/TPC.18.00617.

Rey, P., B. Gillet, S. Römer, et al. 2000. "Over-Expression of a Pepper Plastid Lipid-Associated Protein in Tobacco Leads to Changes in Plastid Ultrastructure and Plant Development Upon Stress." *Plant Journal* 21, no. 5: 483–494. https://doi.org/10.1046/j.1365-313x.2000.00699.x.

Rodriguez-Concepcion, M., J. Avalos, M. L. Bonet, et al. 2018. "A Global Perspective on Carotenoids: Metabolism, Biotechnology, and Benefits for Nutrition and Health." *Progress in Lipid Research* 70: 62–93. https://doi.org/10.1016/J.PLIPRES.2018.04.004.

Rodríguez-Concepción, M. 2010. "Supply of Precursors for Carotenoid Biosynthesis in Plants." *Archives of Biochemistry and Biophysics* 504, no. 1: 118–122. https://doi.org/10.1016/j.abb.2010.06.016.

Romer, J., K. Gutbrod, A. Schuppener, et al. 2024. "Tocopherol and Phylloquinone Biosynthesis in Chloroplasts Requires the Phytol Kinase VITAMIN E PATHWAY GENE5 (VTE5) and the Farnesol Kinase (FOLK)." *Plant Cell* 36, no. 4: 1140–1158. https://doi.org/10.1093/PLCELL/KOAD316.

Rottet, S., J. Devillers, G. Glauser, V. Douet, C. Besagni, and F. Kessler. 2016. "Identification of Plastoglobules as a Site of Carotenoid Cleavage." *Frontiers in Plant Science* 7: 1855. https://doi.org/10.3389/FPLS.2016.01855.

Solymosi, K., and H. Aronsson. 2013. "Etioplasts and Their Significance in Chloroplast Biogenesis." *Advances in Photosynthesis and Respiration* 36: 39–71. https://doi.org/10.1007/978-94-007-5724-0_3.

Takemura, M., and N. Misawa. 2021. "Carotenoid Biosynthesis in Liverworts." *Advances in Experimental Medicine and Biology* 1261: 115–119. https://doi.org/10.1007/978-981-15-7360-6_9.

Torres-Montilla, S., and M. Rodriguez-Concepcion. 2021. "Making Extra Room for Carotenoids in Plant Cells: New Opportunities for Biofortification." *Progress in Lipid Research* 84: 101128. https://doi.org/10.1016/j.plipres.2021.101128.

Van Wijk, K. J., and F. Kessler. 2017. "Plastoglobuli: Plastid Microcompartments With Integrated Functions in Metabolism, Plastid Developmental Transitions, and Environmental Adaptation." *Annual Review of Plant Biology* 68: 253–289. https://doi.org/10.1146/ANNUREV-ARPLANT-043015-111737.

Vergara-Cruces, Á., I. Pramanick, D. Pearce, et al. 2024. "Structure of the Plant Plastid-Encoded RNA Polymerase." *Cell* 187, no. 5: 1145–1159. https://doi.org/10.1016/j.cell.2024.01.036.

Vidi, P. A., F. Kessler, and C. Bréhélin. 2007. "Plastoglobules: A New Address for Targeting Recombinant Proteins in the Chloroplast." *BMC Biotechnology* 7: 4. https://doi.org/10.1186/1472-6750-7-4.

Xu, L., and D. Geelen. 2018. "Developing Biostimulants From Agro-Food and Industrial by-Products." *Frontiers in Plant Science* 9: 1567. https://doi.org/10.3389/FPLS.2018.01567.

Zheng, H., S. Torres-Montilla, X. Huang, M. Rodríguez-Concepción, and S. Lu. 2025. "STAY-GREEN Overexpression in Dark-Incubated Leaves Promotes the Formation of Transitional Chromoplast-Like Plastids." *Plant Physiology* 198, no. 2: kiaf242. https://doi.org/10.1093/PLPHYS/KIAF242.

Zhou, X., S. Rao, E. Wrightstone, et al. 2022. "Phytoene Synthase: The Key Rate-Limiting Enzyme of Carotenoid Biosynthesis in Plants." *Frontiers in Plant Science* 13: 84720. https://doi.org/10.3389/FPLS.2022.884720.

Supporting Information

Additional supporting information can be found online in the Supporting Information section. **Figure S1:** Effect of different compounds on seedling pigmentation. **Figure S2:** X57 treatments leads to increased carotenoid/chlorophyll ratio. **Figure S3:** X57 acts in a dose-dependent manner. **Figure S4:** X57-induced PG proliferation can be followed using the FBN7a-YFP marker protein. **Figure S5:** General overview of the pathways involved in plastidial isoprenoid metabolism. **Figure S6:** BLASTp analysis of Marchantia polymorpha sequences showing homology to tocopherol biosynthesis enzymes. **Table S1:** Accessions and TPM values of genes involved in plastidial isoprenoid metabolism. **Table S2:** Primers used for the qPCR analysis in this study.